2007 IEEE International Conference on
Robotics and Automation
Roma, Italy, 10-14 April 2007

An Ultrasound Probe Holder for Image-Guided Robot-Assisted Prostate Brachytherapy

Basem Yousef, Rajni Patel and Mehrdad Moallem

Abstract—**An ultrasound probe holder is designed for use in the prostate brachytherapy procedure. The holder comprises a passive-jointed stabilizer that can be used to position, manipulate and lock in place the ultrasound probe, and a tracker mechanism to provide the position and orientation of the probe in 3D space. The information obtained from the integrated stabilizer-tracker mechanism can be utilized in image-guided robot-assisted prostate brachytherapy procedures. Performance tests show that the tracker assembly can acquire the position and orientation of the ultrasound probe with an average displacement accuracy of 0.66 mm and roll, pitch and yaw angular accuracies of 0.24º, 0.38º and 0.19º, respectively.**

I. Introduction

PROSTATE cancer is the most common cancer among men. It is the second major cause of death due to cancer in men in North America. The Canadian Cancer Society estimated that in 2006, more than 20,000 men would have been diagnosed with prostate cancer in Canada and more than 4000 would die from it [1].

Among the few options for the treatment of prostate cancer, prostate brachytherapy has proven very effective and successful and thus, has been increasing in popularity. In this manually performed procedure (Fig. 1), radioactive seeds are permanently implanted into the prostate to irradiate the prostatic tumor. Prostate brachytherapy is a two-stage procedure: In the first stage, using a transrectal ultrasound (US) probe to scan the prostate, the cancerous tumor locations, also called "cold spots", are identified and seed implantation into the prostate is planned by the surgeon to form a three dimensional grid. After 2 to 4 weeks, the surgeon performs the second stage during which manual seed implantation is carried out based on the plan.

Since the success of the procedure depends heavily on the accuracy of the seed implantation, many research groups have tried to improve the outcome of the procedure by developing robotic systems that can autonomously or semi-autonomously perform the seed implantation stage taking advantage of the capability of robots to perform high precision and fatigue free movements with accuracy that is beyond that of a human.

Ng et al. [2] used a modular robotic platform for seed implantation for prostate cancer. Phee et al. [3] developed a robotic system for accurate and consistent insertion of a percutaneous biopsy needle into the prostate. Wei et al. [4] used an industrial robot to test the performance of a robot-assisted 3D-transrectal ultrasound guided prostate brachytherapy. Another micro manipulator for percutaneous needle insertion is reported in [5]. At the Urology Robotics Laboratory at Johns Hopkins, several robotic systems have been developed for use in prostate brachytherapy and other procedures. For instance, the (Percutaneous Access of the KidneY (PAKY) needle driver [6] and the Remote Center of Motion (RCM) robot [7] have been developed. While the PAKY consists of a passive arm and a novel needle insertion mechanism, which can accurately introduce a needle into the kidney, the RCM allows for precise needle insertion under radiological guidance. Other urological robots developed in the laboratory are described in [8].

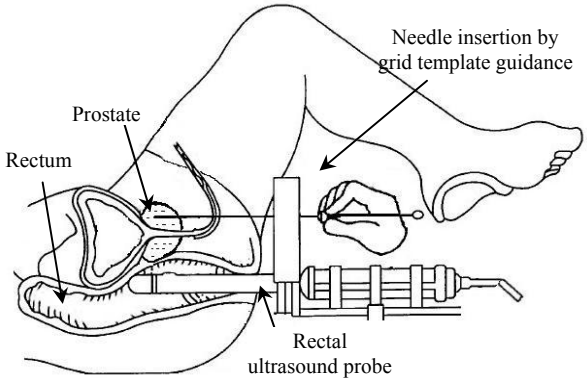

Fig. 1. The current prostate brachytherapy is a manual seed implantation into the prostate [9].

Since a majority of prostate brachytherapy treatments, manually performed or robot-assisted, are carried out under US image guidance, the US probe which is one of the primary tools needed for the procedure, is mounted on a holder, also called a stabilizer, that is used to manipulate, position and lock the probe in place. Moreover, for robot-assisted guidance, it is important to know the position of the US probe relative to the patient to precisely implant the radioactive seeds at pre-selected locations in the prostate as planned by the surgeon. Therefore, another apparatus is needed to provide the location of the US probe relative to the patient.

Different types of US probe stabilizers and precision steppers have been designed such as the mechanisms presented by Ellard et al., who designed the stabilizer assembly described in [10], and a US probe stepper apparatus [11]. Also, Whitmore et al. designed another US stepping device as described in [12].

This research was supported by the Natural Sciences and Engineering Research Council (NSERC) of Canada under the Collaborative Health Research Projects Grant # 262583-2003.

The authors are with the Department of Electrical & Computer Engineering, University of Western Ontario, London, Ontario, Canada N6A5B9; email addresses: byousef2@uwo.ca, rajni@eng.uwo.ca, mmoallem@engga.uwo.ca.

Moreover, real time three-dimensional imaging apparatus and techniques have been developed in an attempt to enable performing on line dynamic seed location planning during the implantation procedure. As described in [13], [14] and [15], a 3D US image can be constructed from a series of 2D US images.

These advances in US imaging and robotic systems can be utilized to perform improved image-guided robot-assisted prostate brachytherapy which may lead to more accurate and convenient ways of delivering the radioactive seeds, thus translating into improved clinical outcomes, reduced side effects, and reduced radiation exposure time.

However, automating image-guided therapy and registering a medical image to the patient requires knowledge of the locations of both the medical image source (e.g., ultrasound) and the robot end-effector, with respect to a global coordinate system that is known relative to the patient. In order to achieve this, it is essential to unify the coordinate systems of the robot end effector frame and the image source (e.g. US probe) frame in order for the robot to know its target point inside the patient through the US image. For example, referring to the schematic diagram in Fig. 2, the robot can find its target point in the goal frame {G} provided that: (1) the relationship between the tool frame {T} and the station frame {S} is known, (note that this can be easily obtained from the kinematic equations of the robot); (2) the goal frame {G} is known with respect to the US probe frame {P}, (again this can be provided by the ultrasound imaging software); and (3) frame {P} must be known with respect to frame {S}. Satisfying the 3rd requirement entails the use of a US probe holder that is equipped with position sensors, which can acquire the position and orientation of the probe. Unfortunately, neither the available stabilizers nor the stepper apparatus can acquire this information, and although some available steppers enable precise US probe motion and rotation [11], [12], the probe's location is still unknown relative to a reference coordinate system. The lack of this information could hamper efforts to automate the manually performed brachytherapy procedure, which can be significantly improved by taking advantage of the use of robots. Moreover, the bulky structures of the available stabilizers increase the potential for robot-robot collisions and occupy a large space in the limited workspace of the brachytherapy procedures.

This paper presents a novel design of a compact size, pre-calibrated ultrasound probe holder that can be used to easily manipulate, position and lock-in-place as well as to provide the location and orientation of the probe relative to a chosen reference coordinate frame on the operating table. This enables a robot in image-guided robot-assisted prostate brachytherapy to find its target point inside the prostate.

Also, we present a practical concept to accurately track an object's position and orientation in 3D space. Our approach overcomes the problems associated with tracking an object by other means. For instance, in an environment with metallic components, the accuracy of electromagnetic trackers decreases due to distortion of the electromagnetic field, and in the case of optical trackers, due to the light reflection off the metal surfaces. Also, direct installation of position sensors (encoders) on a mechanism's joints is difficult in the case of one or more ball joints, and infeasible in the case of having a mechanism with a large number of joints.

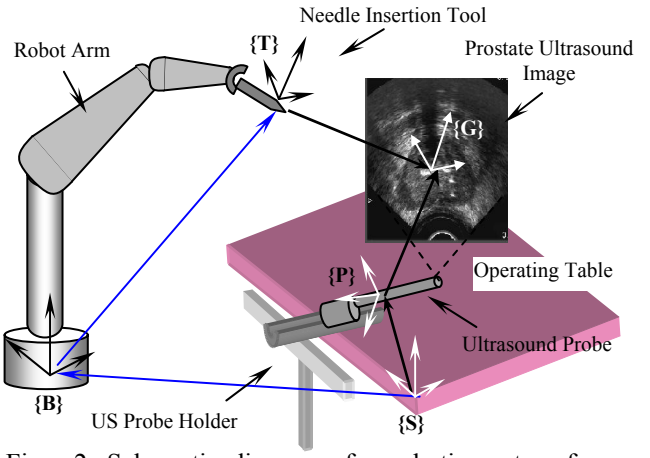

Fig. 2. Schematic diagram of a robotic system for image-guided robot-assisted brachytherapy.

The following sections describe in detail the different components and features of the design.

II. Mechanism Description

The proposed ultrasound (US) probe holder comprises two mechanisms (Fig. 3): a sturdy stabilizer and a position and orientation tracker. Although coupled together as one integrated mechanism, each mechanism can be used independently. The stabilizer joints are loosened to freely manipulate and insert the US probe into the patient's rectum, where the loose-jointed tracker follows the stabilizer and records the probe's final position and orientation through its encoders regardless of the link arrangement and pose of the stabilizer.

A. Stabilizer Design

Fig. 3 shows a CAD model of the stabilizer that consists of 5 links connected by 6 ball joints, which can be manually locked by tightening a lube knob for each of them. Each ball joint consists of a ball and socket at one end, and a revolute joint at the other end as shown in Fig. 3. One can notice that the stabilizer is symmetric with 3 ball joints on each side. Although one side is sufficient to carry and lock the US probe in position, the use of two sides strengthens the structure and makes it sturdier which is essential for robotic applications.

The stabilizer is attached to the operating table through a 4-flange structure, which is permanently bolted to the operating table. Since it is desirable to be able to remove the mechanism for sterilization or to free the operating table for other procedures and to allow for accommodating different surgical tools/equipment necessary for other procedures, the stabilizer is attached to the flange structure through two

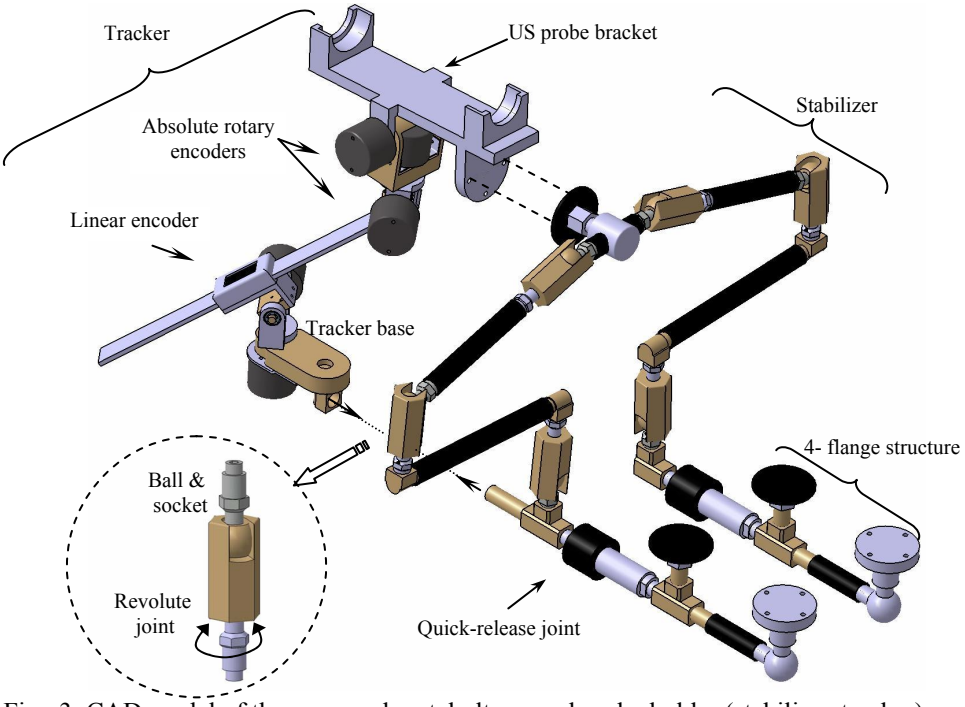

Fig. 3. CAD model of the proposed rectal ultrasound probe holder (stabilizer-tracker) mechanism.

quick-release joints to enable attaching it to and detaching it from the operating table in a very short time, typically 1-2 minutes by one person. This feature is advantageous compared to other stabilizers/holders that need 2 to 3 persons to set up and takes considerably longer set up time.

The US probe mounts on a specially customized bracket, which is attached to the stabilizer structure. When the lube knobs on the ball joints are loose, the surgeon can easily and smoothly manipulate the position and orientation of the probe and then tightening it to lock the probe at the desired position. This architecture allows free motion in 6 degrees of freedom thus enabling insertion of the probe into the patient's rectum freely without applying any force that may result in tearing the inner wall of the rectum or causing trauma to the patient.

A. Tracker Design

The tracker consists of lower-joint and upper-joint assemblies as shown in Fig. 4. While the lower-joint assembly is attached to the tracker base, which is rigidly tightened to the stabilizer (Fig. 3 and 6), the upper-joint assembly is attached to the US probe bracket. It should be noted that the tracker base position and orientation are fixed with respect to the holder flange-structure, and thus to the operating table. The two joint-assemblies are connected by a linear position sensor (encoder) that measures the distance between them.

The lower joint assembly which allows free rotations about two axes is equipped with two absolute rotary encoders that can read the rotational angles θ_1 and θ_2 of the linear encoder stick with respect to the tracker base, i.e., with respect to an arbitrary origin frame affixed to the operating table. The linear distance, L_3, from the tip of the stick to the lower joint is provided by the linear encoder.

The upper joint assembly which allows free rotations about three axes is equipped with three absolute rotary encoders that can read the rotations θ_3, θ_4 and θ_5 about these axes, thus providing the orientation of the US probe bracket with respect to the linear encoder stick.

The information acquired by the 5 rotary encoders and the linear encoder can be utilized to calculate the position and orientation of the US probe with respect to an arbitrary origin frame on the operating table as follows:

Coordinate frames are attached to each encoder to read the rotational angles of the joints, and intermediate frames are used to extract the offset distances of the joint assemblies and part thicknesses, e.g., frames 6, 8 and 9. The frame assignment shown in Fig. 4 is used to generate the Denavit-Hartenberg (D-H) parameters given in Table I that are used to derive the forward kinematics equations [16] that describe the position and orientation of any frame affixed at an arbitrary point on the holder bracket with respect to the origin frame on the operating table. For example, Fig. 4 can be used to obtain the position and orientation of frame {9} with respect to frame {0}, which is known relative to a frame {origin} on the table.

The stabilizer is gaining its high dexterity from its ball joints, but unfortunately, since it is very difficult to install position sensors on ball joints, this makes tracking the end effector of any mechanism that adopts ball joints extremely difficult, thus making these mechanisms useless for the applications where knowledge of the end effector position and/or orientation is needed. The tracker presented in this paper can be used not only with our stabilizer, but also with any mechanism/stabilizer of complex design provided that precautions are taken to avoid collisions between the two mechanisms.

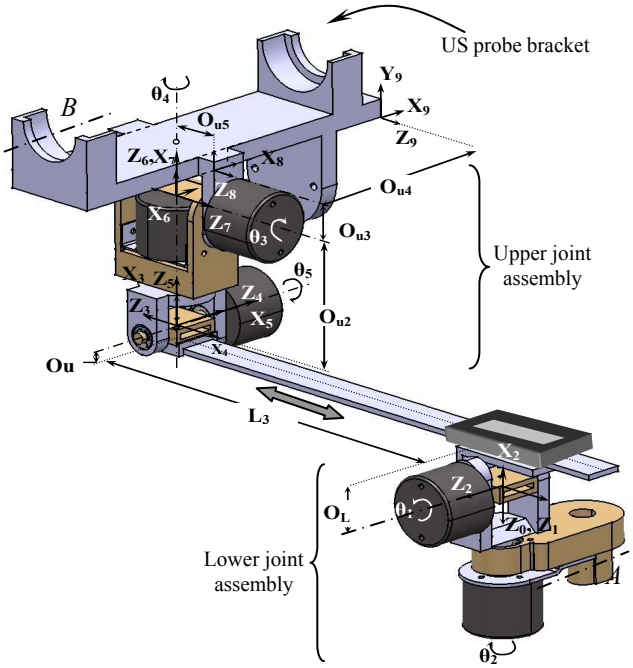

Fig. 4. The tracker assembly and the frame assignment used to derive the forward kinematics equations of the tracker.

TABLE I
THE DENAVIT-HARTENBERG PARAMETERS USED FOR THE DERIVATION OF THE FORWARD KINEMATICS EQUATIONS

i	α_{i-1}	a_{i-1}	d_i	θ_i
1	0	0	0	θ_2
2	$-\pi$	0	0	$\pi+\theta_1$
3	$-\pi$	O_L+O_u	L_3	0
4	$-\pi$	0	0	$\pi+\theta_5$
5	π	0	0	$\pi-\theta_4$
6	0	0	O_{u2}	0
7	π	0	0	$\pi-\theta_3$
8	0	O_{u3}	O_{u5}	$-\pi$
9	0	O_{u4}	0	0

B. Tracker Calibration

Since the tracker base frame is fixed with respect the operating table, the tracker sensors are calibrated with respect to the base frame. Thus, the flange structure should be bolted to the operating table such that the tracker base upper and side surfaces are parallel to those of the operating table. However, "first-time" calibration of the tracker requires knowledge of the encoder readings that correspond to the zero angles according to the D-H parameters in Table I; this is achieved by: 1) locking the tracker firmly in the pose depicted in Fig. 4, i.e. (a) the linear encoder stick and the US probe bracket must be parallel to the tracker base; (b) axis *B* and, θ_1 or θ_5 axes must be parallel to axis *A* (Fig. 4); and (c) θ_4 axis must be perpendicular to the US probe bracket; 2) obtaining the readings of the encoder that correspond to this tracker pose.

In order to achieve the first requirement, two precision *through-all* holes (ϕ 4 mm) are machined in each of the lower and upper joint assemblies with each of the holes passing through all of the components of the joint assembly, such that when precision calibration shafts with the same diameter are tapped into the holes, they accurately lock the tracker in the desired pose allowing the encoder readings to be obtained corresponding to the zero position as per of the D-H parameters table. After the zero-position encoder readings are obtained, the calibration shafts are removed permanently.

C. Materials and Dimensions

To reduce the weight of the holder assembly, the tracker brackets and the holder links are made of aluminum, which resists corrosion as well. Moreover, the ball joints are made of brass that is known for its high corrosion resistance.

Since homing a 6 DOF passive-jointed mechanism is very difficult and requires special software and hardware arrangement, we used absolute encoders at all joints thus allowing the system to be started without additional pre-calibration steps. The encoder at the prismatic joint is a linear digital encoder of 0.01mm accuracy (DIGIMATIC scale unit from Mitutoyo), and the angular sensors are 12-bit rotary encoders (from Gurley Precision Instruments - Model A37).

The dimensions of the links are chosen so that the maximum width of the holder does not exceed the width of most standard operating tables, which is 60 mm. This will free the sides of the operating table and allow for accommodating other equipment that is necessary for the procedure such as the patient's leg supports (Fig. 5), which are needed for the procedure, and also it allows for the use of specially designed robots for the procedure such as the manipulator described in [17] which extends from the side of the operating table.

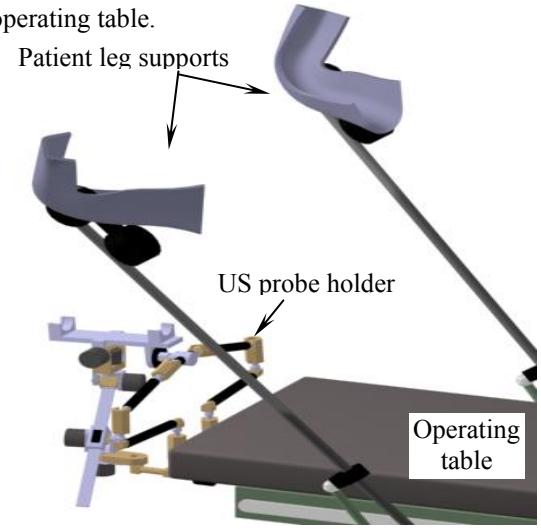

Fig. 5. Probe holder design and dimensions allow for accommodating other mechanisms necessary for prostate brachytherapy such as the leg supports and other robot arms that may extend from the sides.

To verify the machining tolerances and accuracy, all tracker parts dimensions and offset distances were cross-checked using a 0.01 mm accurate digital caliper.

The mechanism's work envelope, which is 250 X 200 X 230 mm, corresponds to 250 mm along the width of the table,

200 mm above the table and 230 mm along the length of the table.

III. Validation and Results

In order to quantify the displacement and angular accuracies of the integrated stabilizer-tracker assembly, the US probe bracket is moved and locked at arbitrary positions and at each position, the actual location and orientation of the bracket are compared against the corresponding "theoretical" location and orientation.

Referring to Fig. 6a, which shows a picture of the actual constructed prototype of the stabilizer-tracker system, in order to obtain the actual location of any point on the bracket, the holder joints are loosened to enable dragging the bracket smoothly and then locking the holder at an arbitrary pose "i". Using a three-axis stage (from Parker Hannifin Co., Irwin, PA) which has an accuracy of 2 μm, the coordinates (x_{ij},y_{ij},z_{ij}) of 3 selected points, typically corners, on the bracket are measured relative to a chosen origin on the operating table (Fig. 6a, 6b) (where i=1,2,…n, denote pose points, and j =1,2,3 are arbitrary points/corners on the bracket). The three points are chosen so that the two edges/lines connecting between them form a right angle. This is because these points are used to define a coordinate frame {act} that will be affixed to the bracket and will be used to define the bracket's actual orientation.

On the other hand, the corresponding theoretical values can be obtained as follows: after reading the joint angles from the encoders, and using the link frame assignment shown in Fig. 4 and the DH parameters (Table I), it is easy to derive both the forward kinematics equations [16] that provide the theoretical locations of the selected points on the bracket based on the encoders angles, and the rotation matrix which can be used to describe the orientation of a frame {theo} that corresponds to the coordinate frame {act}.

When the US probe bracket is at pose "i", the displacement error, E_i, is calculated by

$$E_i = \sqrt{\overline{(\Delta x_i)}^2 + \overline{(\Delta y_i)}^2 + \overline{(\Delta z_i)}^2} \quad (1)$$

where $\overline{(\Delta x_i)}^2 = \frac{1}{3}\sum_{j=1}^{3}(x_{ij} - x_{ij\,theo})$, is the mean of the error in the x-direction for the 3 selected points on the bracket at pose "i".

x_{ij} is the x coordinate of point "j" on the bracket at pose "i" obtained using the three-axis stage.

$x_{ij\,theo}$ is the x coordinate of point "j" on the bracket at pose "i" obtained using the forward kinematics equations.

$\overline{(\Delta y_i)}^2$ and $\overline{(\Delta z_i)}^2$ are calculated similarly.

The mean error, $\overline{E}_t$, for the US probe holder tested at n = 8 locations/poses was calculated using:

$$\overline{E_t} = \frac{1}{n}\sum_{i=1}^{n} E_i \quad (2)$$

The data acquired as described above were used to quantify the angular error as follows:

1) Frame {act} is attached to the bracket with the origin at point 1, where the x-axis, $\hat{x}_{act}$ points in the direction from point 1 to 2, and the y-axis, $\hat{y}_{act}$ points from point 1 to 3. Since points 1, 2 and 3 are selected so that $\hat{x}_{act}$ and $\hat{y}_{act}$ are at right angles, the z-axis direction $\hat{z}_{act}$ can be obtained from the cross product of the vectors defining $\hat{x}_{act}$ and $\hat{y}_{act}$ (Fig. 6b), i.e.

$$\hat{z}_{act} = \hat{x}_{act} \times \hat{y}_{act} \quad (3)$$

Similarly, an imaginary frame {theo} is formed using the theoretical locations of points 1, 2 and 3, which are obtained using the forward kinematics equations [16]. Thus, the axes $\hat{x}_{theo}$, $\hat{y}_{theo}$ and $\hat{z}_{theo}$ of the frame {theo} are defined in the same way {act} is defined. It should be noted that frames {act} and {theo} define the actual and the theoretical orientations, respectively, of the US probe bracket at an arbitrary pose "i".

2) The 3x3 rotation matrices ${}^{o}_{act}R$ and ${}^{o}_{theo}R$ that describe the orientations of frames {act} and {theo} respectively, with respect to the reference frame {origin}, can be obtained by:

$${}^{o}_{act}R = [\,\hat{x}_{act} \quad \hat{y}_{act} \quad \hat{z}_{act}\,] \quad (4)$$

$${}^{o}_{theo}R = [\,\hat{x}_{theo} \quad \hat{y}_{theo} \quad \hat{z}_{theo}\,] \quad (5)$$

Accordingly, the rotation matrix, ${}^{theo}_{act}R$, that describes the orientation of frame {act} with respect to frame {theo} is given by:

$${}^{theo}_{act}R = {}^{o}_{theo}R^{-1}\,{}^{o}_{act}R \quad (6)$$

3) There are many methods [16] that can be used to quantify the angular error of frame {act} with respect to frame {theo}.

We used the "X-Y-Z fixed angles" method, sometimes called the "roll-pitch-yaw angles" in which frame {theo} is fixed and frame {act} is rotated about $\hat{x}_{theo}$ by an angle γ, then about $\hat{y}_{theo}$ an angle β, and finally about $\hat{z}_{theo}$ an angle α. In order to obtain the angles α, β and γ, let the elements of the rotation matrix ${}^{theo}_{act}R$ obtained in (6) be:

$${}^{theo}_{act}R = \begin{bmatrix} r_{11} & r_{12} & r_{13} \\ r_{21} & r_{22} & r_{23} \\ r_{31} & r_{32} & r_{33} \end{bmatrix} \quad (7)$$

then the angles can be calculated by [16]:

$$\beta = A\tan 2(-r_{31}, \sqrt{r_{11}^2 + r_{21}^2}) \quad (8)$$

$$\alpha = A\tan 2(r_{21}/\cos(\beta), r_{11}/\cos(\beta)) \quad (9)$$

$$\gamma = A\tan 2(r_{32}/\cos(\beta), r_{33}/\cos(\beta)) \quad (10)$$

The US probe holder was tested at 8 poses of different positions and orientations. Table II shows that the tracker can perform with high accuracy given by a mean displacement error of $\overline{E_t}$ =0.66 mm, and mean angular errors of $\overline{\alpha}$ =0.24°, $\overline{\beta}$ =0.38° and $\overline{\gamma}$ =0.19°.

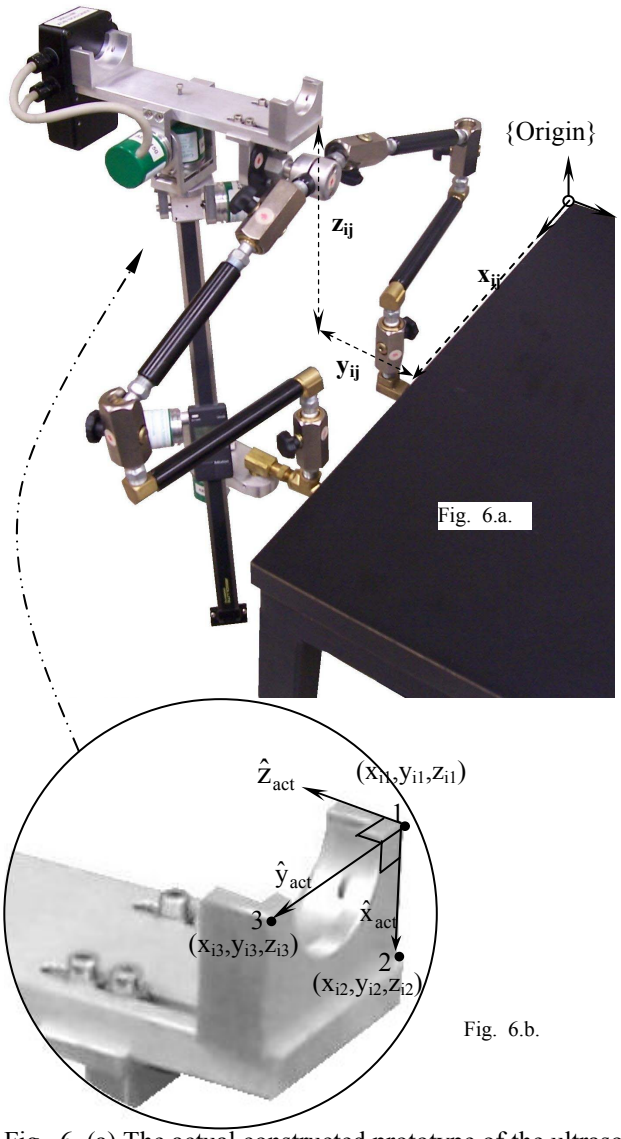

Fig. 6. (a) The actual constructed prototype of the ultrasound probe holder positioned at a target point "i" and the {origin} reference frame is attached to the table. (b) For each point "i", the coordinates of 3 arbitrary points were measured, and the orientation of the end effector is defined by the frame {act} defined by points 1, 2 and 3.

IV. Conclusions

An integrated stabilizer-tracker mechanism has been designed to perform as a holder that can be used to carry, manipulate, lock-in-place, and accurately acquire the position and orientation of an ultrasound probe for use in prostate brachytherapy procedures. A reliable validation technique using forward kinematics was used to evaluate the performance of the holder. The improved sturdiness demonstrated by the compact-sized stabilizer and the high accuracy of the tracking mechanism makes the integrated holder mechanism well suited for use in image-guided robot-assisted prostate brachytherapy. It is anticipated that this will lead to improvement in accuracy and clinical outcomes for the procedure. The novel tracker can also be used to acquire the positions and orientations of other passive mechanisms of complex designs.

TABLE II
The Mean Displacement Error and Angular Errors

i	$\overline{\Delta x_i}$	$\overline{\Delta y_i}$	$\overline{\Delta z_i}$	E_i(mm)	α°	β°	γ°
1	0.14	0.15	0.13	0.24	0.31	0.62	0.28
2	0.43	0.24	0.28	0.57	0.22	0.05	0.21
3	0.63	0.21	0.26	0.71	0.13	0.55	0.25
4	0.61	0.35	0.28	0.76	0.52	0.07	0.03
5	0.10	0.80	0.48	0.94	0.37	0.55	0.06
6	0.30	0.48	0.29	0.64	0.06	0.59	0.23
7	0.24	0.51	0.05	0.57	0.22	0.20	0.23
8	0.12	0.71	0.43	0.84	0.07	0.41	0.20
Mean				**0.66**	**0.24**	**0.38**	**0.19**

References

[1] Online: http://www.cancer.ca/ccs/internet/standard/0,3182,3172_14471_371299_langId-en,00.html.

[2] W.S. Ng, V.R. Chung, S. Vasan and P. Lim, "Robotic radiation seed implantation for prostatic cancer", Proceedings of the 18th Annual International Conference of the IEEE Engineering in Medicine and Biology Society, vol. 1, Nov. 1996, pp. 231-233.

[3] L. Pee, D. Xiao, J. Yuen, C. F. Chan, H. Ho, C. H. Thng, C. Cheng and W.S Ng, "Ultrasound Guided Robotic System for Transperineal Biopsy of the Prostate", Proceedings of the IEEE International Conference on Robotics and Automation, April 2005, pp. 1315-1320.

[4] Z.Wei, G. Wan, L. Gardi, G. Mills, D. Downey and A. Fenster, "Robot-Assisted 3D-TRUS Guided Prostate Brachytherapy: System Integration and Validation", Med. Phys., vol. 31, No. 3, March 2004, pp. 539-548.

[5] H. Bassan, R. V. Patel and M. Moallem, "A Novel Manipulator for Prostate Brachytherapy: Design and preliminary results", Proc. of the 4th IFAC Symposium on Mechatronics Systems, 2006.

[6] J. Cadeddu, D. Stoianovici, R.N. Chen, R.G. Moore and L.R. Kavoussi, "Stereotactic Mechanical Percutaneous Renal Access", *Journal of Endourology*, vol. 12, No. 2, April 1998, pp. 121-126.

[7] D. Stoianovici, J.A. Cadeddu, L.L. Whitcomb, R.H. Taylor and L.R. Kavoussi, "A Robotic System for Precise Percutaneous Needle Insertion", *Thirteen Annual Meeting of the Society for Urology and Engineering*, San Diego, CA, May 1998. .

[8] D. Stoianovici, URobotics - Urology Robotics at Johns Hopkins. *Computer Aided Surgery,* 2001, 6, pp. 360-369.

[9] W. Whitemore, III, W. Barzell and R. Wilson, Omni-Directional Precision Instrument Platform, US patent No.5961527, 1999.

[10] T. Ellard and S. Knudsen, Stabilizer assembly for stepper apparatus and ultrasound probe, US patent No. 6179262, 2001.

[11] Terence R. Ellard, Stepper apparatus for use in the imaging/treatment of internal organs using an ultrasound probe, US patent No. 5871448, 1999.

[12] W. Whitemore, III, W. Barzell and R. Wilson, Ultrasound Probe Support and Stepping Device, US patent No.5931786, 1999.

[13] S. Tong, D Downey, H. Cardinal and A. Fenster, "A three-dimensional ultrasound prostate imaging system," *Ultrasound Med. & Biol.*, vol. 22, No. 6, 1996, pp. 735-746.

[14] E. Burdette and B. Komandina, Radiation Therapy and Real Time Imaging of A patient Treatment Region, US patent 6512942, 2003.

[15] T. Nelson and D. Pretorius, "Three-dimensional ultrasound imaging", Ultrasound Med. Biol., 24, 1998, pp. 1243-70.

[16] John J. Craig, Introduction to Robotics: Mechanics and Control 3rd ed. (Upper Saddle River, N.J.: Pearson Education, 2005).

[17] B. Yousef, R. V. Patel and M. Moallem, "Macro-Robot Manipulator for Medical Applications", IEEE International Conference on Systems, Man and Cybernetics, Oct. 2006.